

Y. H. Choi · H. B. Kim

Pulsating jet control for manipulating the separation bubble behind the fence

Received: 25 August 2008 / Accepted: 17 January 2010 / Published online: 9 March 2010
© The Visualization Society of Japan 2010

Abstract An optimization study of a pulsating jet was performed to manipulate the separation bubble behind the fence. The experiments were carried out in a circulating water channel and the vertical fence was submerged in the turbulent boundary layer. The parameters used for controlling the pulsating jet included the frequency, speed and velocity profile of jet, and the geometries including angle and location of nozzle. In addition, we investigated the effect of upstream boundary layer changed by continuous suction in front of the jet nozzle. Each test case was divided into 20 phases and phase-averaged DPIV method was applied to measure the velocity field. From the results, the main mechanism of reduction of bubble length was the vortex shedding from the recirculating region. The specific jet condition and nozzle geometries which were effective to reduce the separation bubble behind the fence were found.

Keywords Vertical fence wake · Separation bubble · Pulsating jet · Phase-averaged DPIV

1 Introduction

Separated shear flows around surface-mounted obstacles have received considerable attention due to their practical importance. The fence flow is the typical example of separated shear flows around surface-mounted obstacles. The separated shear flow generated from the tip of a vertical fence has various sizes ($9 \sim 15H$) of recirculating flow region behind the fence.

Manipulation of the fence flow can be used for various purposes such as the reduction of drag (Buchheim et al. 1985; Hucho 1998), increasing/decreasing the mixing (Kang and Lee 2008; Badr and Harion 2007), and solving aero-optic problems. (Andino et al. 2007). There exist various classifications for flow-control methods (Gad-el-Hak 2006). One of these is whether the energy consumption is used or not. Flow-control methods were classified into passive and active control using this criterion. The active control method which requires energy consumption is further classified into open-loop or closed-loop methods. The present study was performed by active control with open-loop method. The predetermined control parameter was very important because it could not be changed by the results like feed-forward or feedback control method.

To manipulate the vertical fence flow, some studies using active control methods have been performed. Miau and Chen (1991) investigated the flow control using the oscillating fence. The study was

Y. H. Choi · H. B. Kim
School of Mechanical and Aerospace Engineering, Gyeongsang National University, Jinju, Gyeongnam 660-701, Korea

H. B. Kim (✉)
Research Center for Aircraft Parts Technology, Gyeongsang National University, Jinju, Gyeongnam 660-701, Korea
E-mail: kimhb@gnu.ac.kr
Tel.: +82-55-7516076
Fax: +82-55-7620227

carried out using a hot-wire method in a wind tunnel; phase-averaged technique was applied. They found that a large-scale vortical structure developed with an organized form and that it diffused quickly. Siller and Fernholz (1997, 2007) studied the manipulation of fence wake flow using an oscillating spoiler and acoustic jet device. They presented the optimal frequency of pulsating flow and the distance of nozzle from the fence. They reported that the time-mean length of separation bubble was reduced to 40% of the original uncontrolled case at maximum. Orellano and Wengle (2000, 2001) numerically studied the separation bubble of a surface-mounted fence under a periodic jet in front of the fence by using DNS and LES methods. They used two specific forcing frequencies of pulsating jet. One was from the ‘shear layer type’ instability [Strouhal number (Str_h) = 0.6]; the other was the ‘shedding type’ instability (Str_h = 0.08). This ‘shear layer type’ instability means that the Kelvin–Helmholtz instability of the separated shear layer and ‘shedding type’ instability represent the instability of the entire separation bubble (Sigurdson 1995). In case of backward-facing step flow, it was found that the optimum forcing frequency was heavily related to ‘shear layer type’ instability (Chun and Sung 1996; Wengle et al. 2001). Orellano and Wengle (2000, 2001) showed that the optimal forcing frequency of a pulsating jet is the same as the shedding frequency of the separation bubble in case of the fence; this was the same result as attained by Siller and Fernholz (2007).

In this study, we have performed a further optimization study of pulsating jets for manipulating the separation bubble behind the fence using various parameters. The effect of these parameters included not only previously studied parameters such as the frequency, speed, nozzle distance from the fence, but also the profile of the pulsating jet, angle of nozzle and the change of upstream velocity profile were investigated experimentally. A phase-averaged DPIV method was used and the entire velocity fields were measured at each phase. We believe this study can help the understanding of pulsating jet control for altering the fence wake flow and can be used for validating the computational results.

2 Experimental apparatus and methods

The experiments were performed in a circulating water channel; the size of test section was $300W \times 300H \times 1,000L$ (mm). The schematic diagram of the fence with the coordinate system used in this study and experimental apparatus is shown in Fig. 1. The fence on the plate was located at 500 mm downstream from the entrance of test section. The height (H) of the fence was 15 mm, the width was $20H$ and the thickness was $0.1H$. Fence had a sharp edge tip. The aspect ratio of the fence was 20 and the blockage ratio of this experiment was 5% and the acceleration effect due to the blockage ratio was negligible. The free-stream velocity (U_0) was 0.2 m/s. The Reynolds number based on the height of fence and freestream velocity was 3,000. This was the same Reynolds number used by Orellano and Wengle (2000, 2001).

The tripping wire to make the turbulent boundary layer was located at the entrance of the plate. The slit nozzle of pulsating jet flow was installed in front of the fence. The width of the nozzle was $20H$ and its

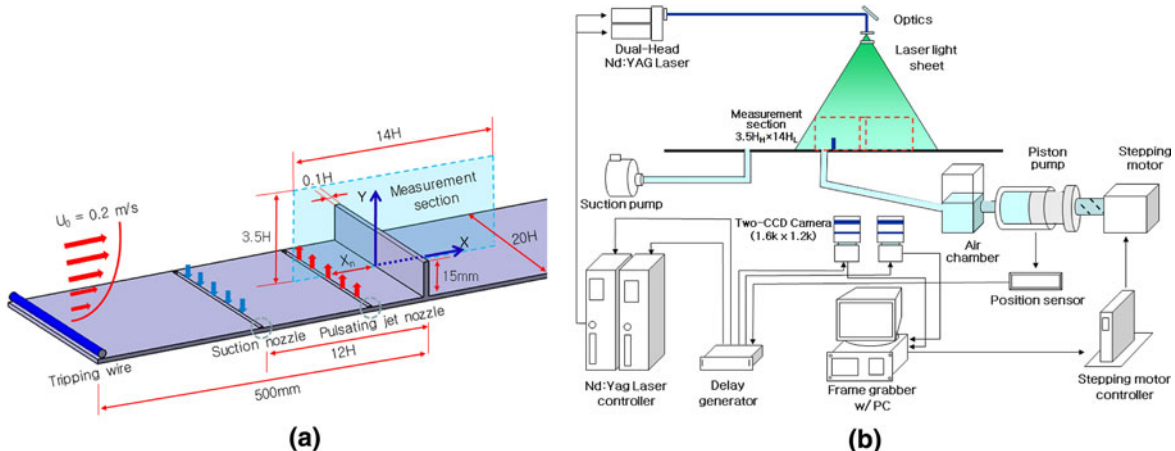


Fig. 1 Schematic diagram of experimental model and apparatus. **a** Fence model with coordinate system. **b** Experimental apparatus

thickness was 1 mm. The location (X_n) of the nozzle was varied from $-0.5H$ to $-3H$ in front of the fence to find the effect of nozzle distance. The pulsating jet was generated by the piston pump precisely controlled by the computer. Although the forcing frequency of the pulsating jet was limited to the lower number, we made various jet profiles using piston pump which is not possible in the acoustic method.

The piston pump, CCD cameras and pulse laser were synchronized by the delay generator. The frequency, vertical jet speed (V_{jet}) and vertical velocity profile of the jet were easily controlled by programming the stepping motor that moves the piston. The air chamber was installed to remove the oscillation of jet flow. The location of the piston was monitored by an optical sensor and this sensor signal was used for triggering the DPIV system including CCD cameras and a laser. Two CCD cameras of $1.6k \times 1.2k$ pixel resolution were used to measure the instantaneous velocity fields around a vertical fence. The size of the measurement region was $14H$ (width) $\times 3.5H$ (height). We used the cross-correlation based DPIV method with window-offsetting to increase the spatial resolution of the instantaneous velocity vectors. The interrogation window was 20×20 pixels with 50% overlapping and a spatial resolution of 1.4×1.4 mm. We used a phase averaging method to investigate the periodic fence wake with time. A single cycle was divided into 20 phases; 200 instantaneous velocity fields were averaged at each phase.

A continuous suction of flow in front of the fence was applied to alter the upstream velocity profile. The suction nozzle had the same geometry as the silt nozzle of the pulsating jet and was located at $12H$ in front of the fence. Due to the suction of the low-speed fluid, the momentum of the boundary layer increased at the fence top position. The boundary layer thickness without the suction is $3.2H$ and $2.3H$ with the suction. The fence was submerged in the boundary layer. In case of previous studies (Siller and Fernholz 2007; Orellano and Wengle 2001), the thickness of the boundary layer was lower than the height of the fence.

3 Results

We experimentally investigated the control of a pulsating jet for manipulating the separation bubble behind the fence in this study. The Strouhal number was defined as ($Str_H = fH/U_0$). V_{jet} is the maximum vertical velocity at one cycle and was varied from 0.5 to $2.0U_0$. The vertical velocity profile of the pulsating jet had smooth sine-wave like velocity profiles. The maximum blowing speed was larger than suction because the shape of the jet passing through the nozzle was different between the blowing and suction phases. During the blowing phase, the pulsating jet had a parabolic profile and in case of suction phases, the shape of the jet had a flat profile. The time-mean length (X_r) of separation bubble of all test cases was non-dimensionalized by the length (X_{r0}) of the uncontrolled fence flow. The reattachment length of the uncontrolled fence flow was measured by ensemble-averaging 1,000 instantaneous velocity fields and found to be $10H$; this was slightly increased to $10.5H$ with the suction of the boundary layer. Experiments to find the effect of the Strouhal number (Str_H), vertical speed of jet (V_{jet}) and position of the nozzle (X_n) were performed at the start. Figure 2 shows the comparison of bubble lengths according to the Strouhal number, the nozzle distance and jet speed. The results were compared with those of Siller and Fernholz (2007). In case of Strouhal number optimization (Fig. 2a), despite the difference of the Reynolds number ($Re = 10,500$ at

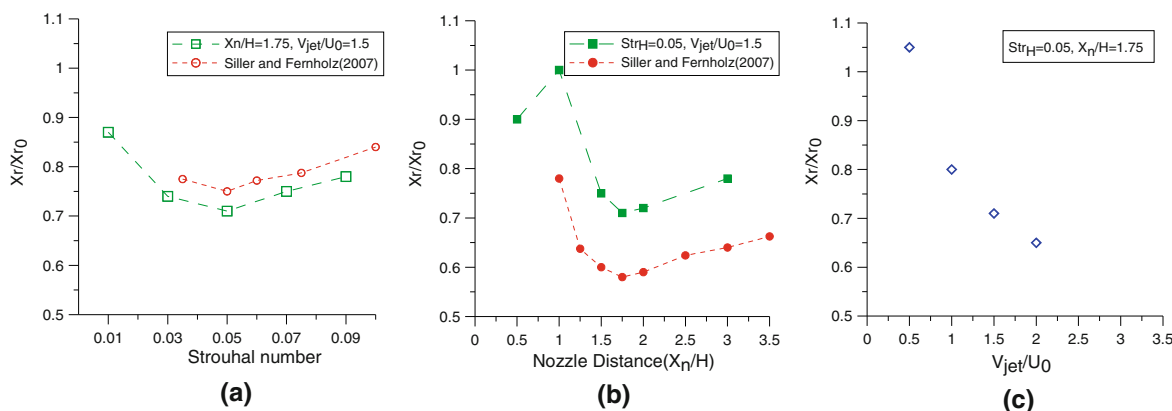


Fig. 2 Non-dimensionalized reattachment length comparison according to the Strouhal number, nozzle distance and jet speed apparatus. **a** Strouhal number optimization; **b** nozzle distance optimization; **c** jet optimization

Siller and Fernholz (2007), upstream velocity profile and jet velocity, the trends are nearly the same as those found in Siller and Fernholz (2007). The maximum reduction of time-mean reattachment length appeared at $Str_H = 0.05$, and as the Strouhal number deviated from this optimal value, the length of separation bubble increased. The distance of nozzle was set at $X_n/H = 1.75$ following Siller and Fernholz (2007). The jet velocity was $V_{jet}/U_0 = 1.5$.

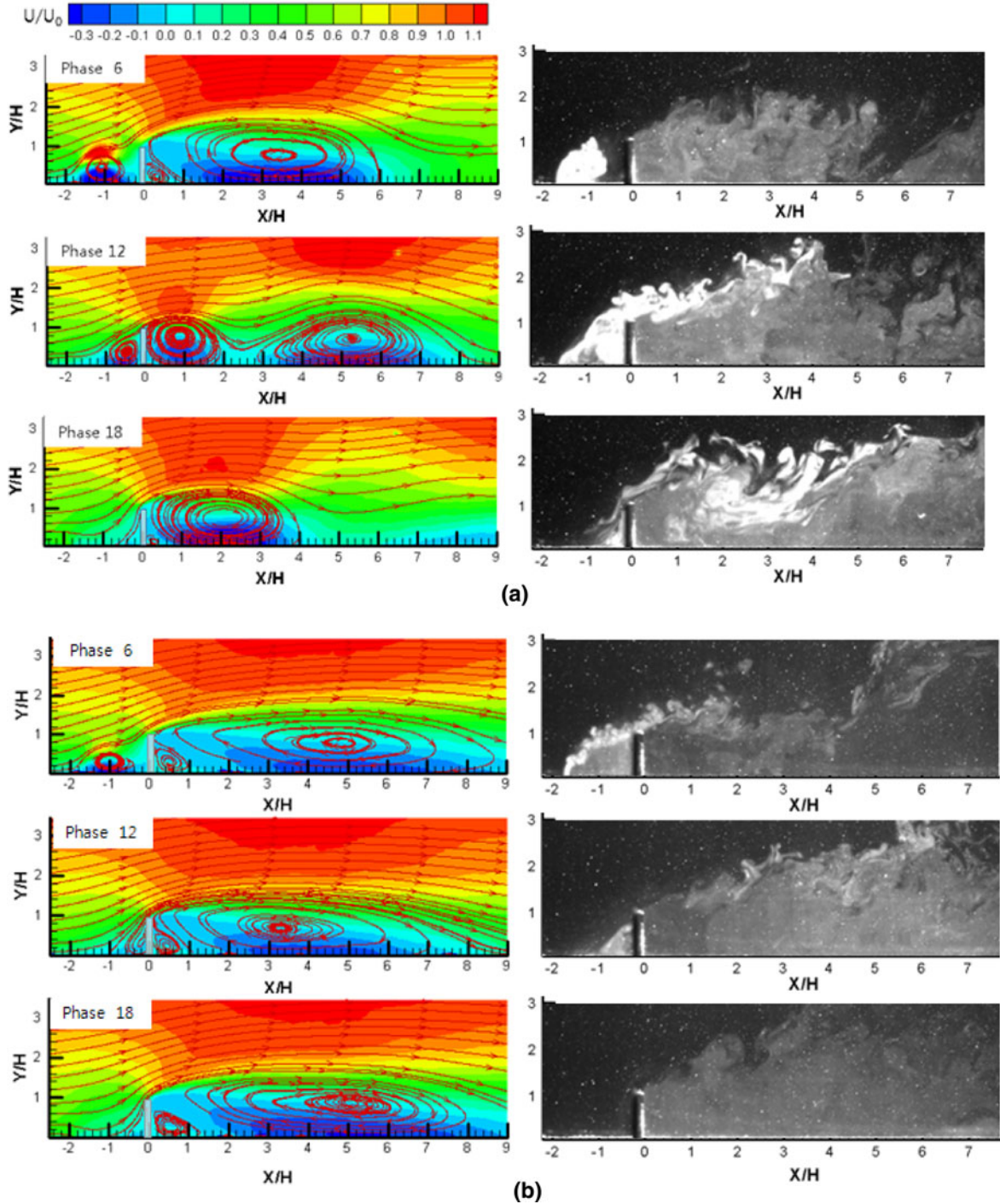


Fig. 3 Comparison of phase-averaged streamwise velocity contours and dye-injection images. **a** $Str_H = 0.05$, $X_n/H = 1.75$, $V_{jet}/U_0 = 2.0$; **b** $Str_H = 0.05$, $X_n/H = 1.75$, $V_{jet}/U_0 = 0.5$

The effect of nozzle distance also showed the same trends as found in the previous study (Fig. 2b). The maximum reduction of time-mean length of separation bubble appeared at $X_n/H = 1.75$. When the distance of nozzle became smaller than $1H$, the reduction of separation bubble also decreased. Especially at $X_n/H = 1$, there was no reduction of separation bubble. We discuss this in detail in a later part of the paper.

In case of vertical speed of the pulsating jet, Fig. 2c shows the continuous reduction of time-mean length of separation bubble as the jet velocity increased. Orellano and Wengle (2001) used a simulated synthetic jet with maximum amplitude of $V_{jet}/U_0 = 0.5$ and they reported a reduction of separation bubble. However, the size of separation bubble slightly increased in the present study at that amplitude.

We compared the phase-averaged velocity field results of these less effective and even reversal cases with the clear reduction cases and found there was no vortex shedding from the separation bubble in this smaller reduction case. The mechanism of reduction of time-mean length of separation bubble was known to be due to the vortex shedding from the separation bubble. Phase-averaged velocity field data in the largest reduction case at the $Str_H = 0.05$, $X_n/H = 1.75$, $V_{jet}/U_0 = 2.0$ and less reduction case at the $Str_H = 0.05$, $X_n/H = 1$, $V_{jet}/U_0 = 1.5$ with dye-injection images are shown in Fig. 3. This clearly shows this shedding process from the separation bubble. In this figure, shedding appeared from the separation bubble due to the strong entrainment by the vortex developed from the pulsating jet. However, in no reduction cases such as $X_n/H = 1$, no vortex shedding occurred.

This optimization study of frequency, speed and nozzle distance effect supports previous studies. We further investigated the effect of the pulsating jet by changing the vertical velocity profile. These profiles have the same Strouhal number and jet velocity. Although the pulsating jet used for optimizing the frequency, speed and jet velocity had zero net mass flux condition, the changed jet profile did not fulfill this zero net mass flux. By using a different stepper motor program, the velocity profile was easily changed and is shown in Fig. 4. The velocity profiles were classified by following the appearance of maximum velocity phases. We changed the peak phase and decreased the length of negative flow phases.

Figure 5 shows a comparison of reduction of separation bubble by changing the velocity profile. Although the maximum reduction appeared at the zero net mass flux profile, the maximum difference was less than 7% and this meant the change of velocity profile was less sensitive to reducing the separation bubble, unlike other parameters such as frequency, speed and nozzle distance. During the experiments, it took time and effort to make a smooth sine-wave-like velocity profile. The results of Fig. 5 show that the necessity of making an exact sine-wave profile was less critical for reducing the separation bubble, that is, it can save time and efforts for making a smooth sine-wave profile of the pulsating jet. Figure 6 shows the results of changing upstream velocity profiles. At the same nozzle distance of $X_n/H = 1.75$, the time-mean length of separation bubble was reduced to 6% of maximum when the suction of the boundary layer was applied.

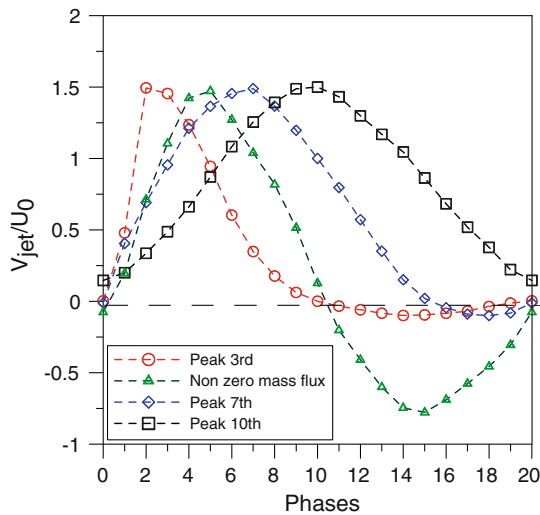


Fig. 4 Various phase-averaged velocity profiles of zero and non-zero net mass flux pulsating jet at $Str_H = 0.05$, $X_n/H = 1.75$, $V_{jet}/U_0 = 1.5$

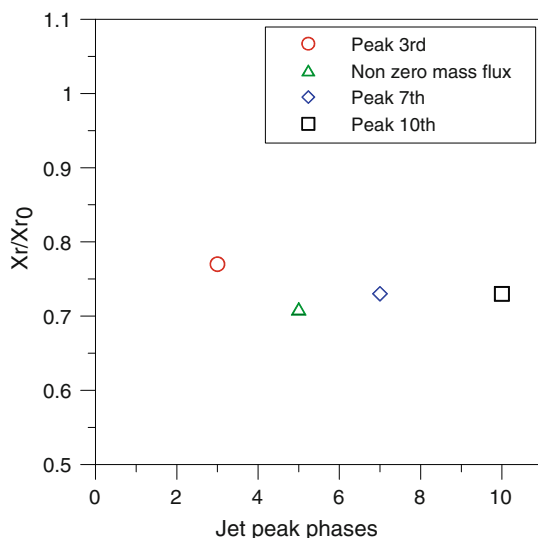


Fig. 5 Non-dimensionalized reattachment length comparison according to the jet velocity profiles

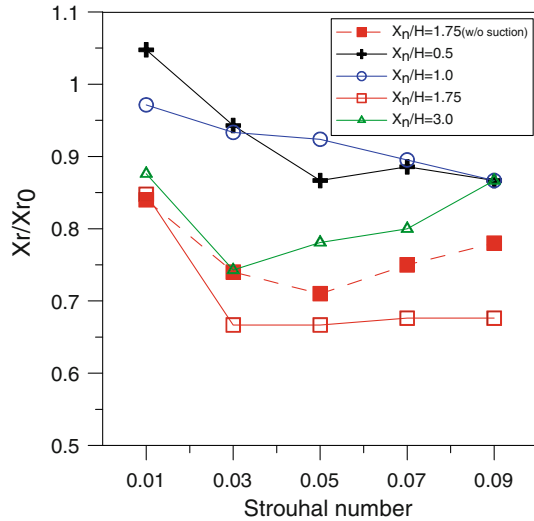


Fig. 6 Non-dimensionalized reattachment length comparison according to the Strouhal number and nozzle distance by changing the upstream boundary layer

The results of Fig. 6 can be classified into two types according to the nozzle distance. When the distance was less than $1H$, the reduction of time-mean length of separation bubble length increased with the increasing Strouhal number. In other cases, there was a value of effective Strouhal number that reduced the separation bubble; this value was 0.03 instead of 0.05 as in the previous results. Phase-averaged velocity data showed that the smaller reduction case had no vortex shedding phenomena from the separation bubble.

The effect of nozzle angle was also investigated. The location of nozzle was at $1.75H$ in front of the fence and the jet parameters were at $Str_H = 0.05$ and $V_{jet}/U_0 = 1.5$. The experiments were performed while increasing the angle of the nozzle from -45° to 45° at a 15° interval. The clockwise direction was positive. The result is shown in Fig. 7. The largest reduction appeared when the jet was injected at -30° in the opposite direction of the upstream flow. The counter-clockwise rotation of the nozzle was less sensitive for reducing the separation bubble; the maximum difference of reduction between -30° and 0° was just 6%. However, if the angle of nozzle rotated above 0° , the reduction of separation bubble quickly disappeared. A 15° increase from 0° brought an 18% increase of the time-mean length of separation bubble.

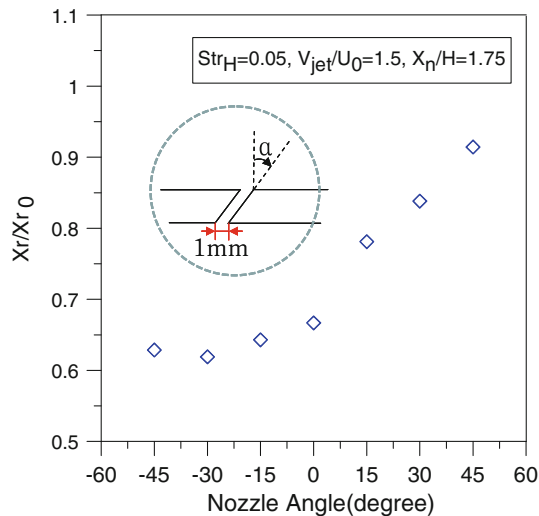


Fig. 7 Non-dimensionalized reattachment length comparison according to various nozzle angles

This result was related to the development of a vortex in front of the fence. Figure 8 shows the dye-injection results and swirling strength comparison at different angles, which have larger or smaller reduction of the separation length. Swirling strength is one of the metrics to define the vortex and has a large and negative value in regions that are rotating more than shearing or diverging (Vollmers 2001; Chakraborty et al. 2007). At the same jet parameters such as the speed, Strouhal number, and nozzle distance, the vortex generated by the pulsating jet was different according to the nozzle angle. As the angle increased above 0° , the vortex did not develop and the reduction of the separation bubble decreased.

This result confirmed the importance of vortex generation for reducing the time-mean length of separation bubble.

Figure 9 shows the change of length of separation bubble as the phases change when the reduction was larger or smaller. When the reduction was larger, there was a steep decrease of reattachment length due to the vortex shedding phenomena from the separation bubble. In case of less reduction, there was no steep change of length and the recirculation bubble oscillates within one cycle. In addition, this figure also showed that the entrainment of fluid by a weak vortex made the size of the separation bubble larger than that in uncontrolled case.

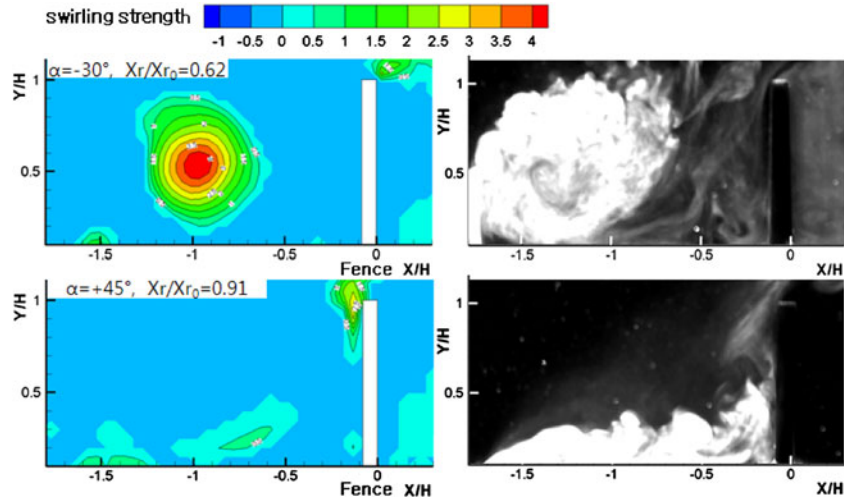


Fig. 8 Comparison of swirling strength and dye-injection images according to various nozzle angles

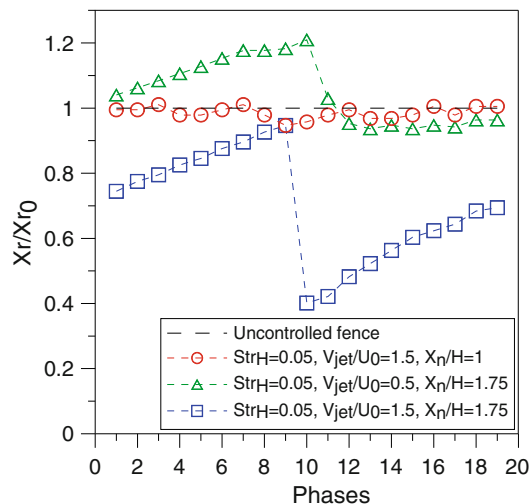


Fig. 9 Comparison of non-dimensionalized reattachment length according to the phase change

4 Conclusion

In this study, we investigated the effect of a pulsating jet for manipulating the separation bubble behind the fence. There was a specific frequency, distance and angle that achieved the largest reduction of time-mean length of separation bubble.

The maximum reduction appeared when Strouhal number was 0.05 and the nozzle distance was $1.75H$ with -30° blowing angle of jet flow. The parametric studies of frequency and jet speed reveals there are universal optimal values. In addition, these values strongly depend on the upstream velocity condition and the change of jet profiles is less effective to reduce the separation bubble. We showed that the main cause of reduction was the vortex shedding phenomena from the separation bubble; this separation was governed by the vortex developed from the pulsating jet. If the vortex was weak and there was no separation from the bubble, the reduction of the bubble became smaller. The separation bubble can become even bigger than the uncontrolled fence flow under specific conditions.

Acknowledgments This work was supported by Priority Research Centers Program (2009-0094016) and the Pioneer Research Center Program (2009-0082813) through the National Research Foundation of Korea(NRF) funded by the Ministry of Education, Science and Technology.

References

- Andino M, Wallace R, Schmit R, Camphouse R, Myatt J., Glauser M (2007) Effects of flow control over a 3D turret. In: Proc 60th annual meeting of the division of fluid dynamics, Salt Lake City
- Badr T, Harion LL (2007) Effect of aggregate storage piles configuration on dust emission. *Atmos Environ* 41:360–368
- Buchheim R, Marketzke J, Piatek R (1985) The control of aerodynamic parameters influencing vehicle dynamics. SAE No.850279, SAE, Warrendale
- Chakraborty P, Balachandar S, Adrian RJ (2007) Kinematics of local vortex identification criteria. *J Vis* 10:137–140
- Chun KB, Sung HJ (1996) Control of turbulent separated flow over a backward-facing step by local forcing. *Exp Fluids* 21:417–426
- Gad-el-Hak M (2006) Flow control: passive, active and reactive flow management. Cambridge, New York
- Hucho W (1998) Aerodynamics of road vehicles: from fluid mechanics to vehicle engineering. SAE, Warrendale
- Kang JH, Lee SJ (2008) Mechanical response of young canes of wind-blown Kiwifruit vines. *J Vis* 11:231–238
- Miau JJ, Chen MH (1991) Flow structures behind a vertically oscillating fence immersed in a flat-plate turbulent boundary layer. *Exp Fluids* 11:118–124
- Orellano A, Wengle H (2000) Numerical simulation (DNS and LES) of manipulated turbulent boundary layer flow over a surface-mounted fence. *Eur J Mech-B/Fluids* 19:765–788
- Orellano A, Wengle H (2001) POD analysis of coherent structures in forced turbulent flow over a fence. *J Turbul* 2:2–35
- Sigurdson LW (1995) The structure and control of a turbulent reattaching flow. *J Fluid Mech* 298:139–165
- Siller HA, Fernholz HH (1997) Control of the separated flow downstream of a two-dimensional fence by low-frequency forcing. *Appl Sci Res* 57:309–318
- Siller HA, Fernholz HH (2007) Manipulation of the reverse-flow region downstream of a fence by spanwise vortices. *Eur J Mech-B/Fluids* 26:236–257
- Vollmers H (2001) Detection of vortices and quantitative evaluation of their main parameters from experimental velocity data. *Meas Sci Tech* 12:1199–1207
- Wengle H, Huppertz A, Barwolff G, Janke G (2001) The manipulated transitional backward-facing step flow: an experimental and direct numerical simulation investigation. *Eur J Mech-B/Fluids* 20:25–46